Elementary-flux-pinning potential in type-II superconductors

E. V. Thuneberg
*Research Institute for Theoretical Physics, Siltavuorenpenger 20C, SF-00170 Helsinki, Finland**
and Nordisk Institut for Teoretisk Atomfysik (NORDITA), Blegdamsvej 17, DK-2100 Copenhagen Ø, Denmark

J. Kurkijärvi
Department of Technical Physics and Low Temperature Laboratory, Helsinki University of Technology, SF-02150 Espoo, Finland

D. Rainer
Physikalisches Institut der Universität Bayreuth, Universitätsstrasse 30, D-8580 Bayreuth, West Germany
(Received 31 October 1983)

Flux pinning brought about by quasiparticle scattering off small-spatial-extent defects is studied using the quasiclassical method. The theory as applied to the pinning problem is presented in detail and an efficient method is given for solving the transportlike equation of the theory numerically. The pinning potential of a model impurity with hard-sphere—scattering phase shifts is computed over the entire temperature range in a pure superconductor with the Ginzburg-Landau parameter $\kappa=0.9$. The pinning energies arising from quasiparticle scattering turn out to be up to 2 orders of magnitude larger than those predicted by the traditional theory for small-spatial-extent pinning centers.

I. INTRODUCTION

Flux pinning is of great practical importance since it determines the critical current of a type-II superconductor in a magnetic field. As soon as the flux-line lattice begins to move, pushed by a current through the sample, an electric field arises leading to dissipation. Flux lines tend to stick to various defects of the metal lattice such as impurities, dislocations, grain boundaries, voids, etc.

It is hard to set up a general quantitative theory of the maximum current that leaves the flux lattice stationary in the background of imperfections of some given distribution. The problem has two separate aspects. First, one has to know the interaction between a flux line and a single defect which is often called the elementary pinning force. Second, it is a complicated matter to decide how the elementary pinning forces add up to a holding force on the elastic flux lattice accommodating itself to the presence of the impurities. The latter dilemma is referred to as the summation problem,[1-3] and its nature is well illustrated by the rather trivial observation that a random distribution of defects does not pin a rigid-vortex lattice at all whatever the elementary pinning potential.

In this paper we address ourselves to the elementary pinning force. We show that there is a strong pinning mechanism[4] brought about by quasiparticle scattering off the pinning center. Traditionally, it is assumed that a void or similar defects pin because they prohibit superconducting condensation in their locality. Hence a void attracts normal regions such as a vortex core in order to avoid the loss of condensation energy.[2,5] Elementary pinning energies from this source are on the order of the condensation energy density $\frac{1}{2}\mu H_c^2$ times the volume of the pinning center $\frac{1}{6}\pi d^3$, and a more sophisticated calculation can only supply a multiplicative factor not much different from unity. The quasiparticle scattering effect considered in this paper pins stronger by 1 or 2 orders of magnitude in the case of small defects, $d \ll \xi_0$. The physical basis of the new mechanism is a nonlocal effect that a scattering center has on Cooper pairs in its immediate environment. A scattering center helps a superconductor to sustain deformations of the order parameter up to distances on the order of the zero-temperature coherence length ξ_0. Hence it is energetically advantageous for a region where the order parameter varies strongly, e.g., a vortex core, to coincide with a scattering center. In the case of small impurities of size d, in particular, the new mechanism leads to elementary pinning energies proportional to $\mu H_c^2 \xi_0 d^2$, larger by the factor ξ_0/d than the $\mu H_c^2 d^3$ from the excluded volume effect.

It is clear that accurate information is needed on the elementary pinning force in order to experimentally test a summation theory. It has been a long-standing puzzle that no summation theory has been able to account for the relatively high critical currents measured.[1] The present calculation removes that difficulty and we hope that having brought the small-defect elementary pinning force under control will make possible definite quantitative comparisons of summation theories[6,7] with experiment.[8]

The quasiparticle scattering mechanism of pinning is not contained in the conventional Ginzburg-Landau theory for small defects. (For large defects the application of the proper boundary condition on the surface of the defect would automatically include the present effect. Then it would not be the largest contribution.) Evaluating the small defect pinning potential, we apply the quasiclassical method.[9,10] The quasiclassical method is equivalent to the WKB method of quantum mechanics. It is an improve-

ment on the old BCS-Gorkov theory in the same sense as ray tracing is an improvement on the full problem of the wave equation. In the latter the unnecessary information on the scale of the wavelength of light is eliminated before attacking the problem. The propagation of light rays through surfaces can then be described simply in terms of indices of refraction. In superconductivity, experimentally interesting length scales are on the order of the BCS coherence length ξ_0. Any information on the scale of k_F^{-1} included in the theory is unnecessary and indeed unjustified in the BCS framework. The present calculation would not be feasible without this essential simplification of the BCS-Gorkov method. We use Eilenberger's[9] formulation of the quasiclassical method in terms of ξ-integrated Green's functions. The scattering properties of the defect are described in terms of scattering phase shifts, and those of the hard sphere are used as an illustration. There are no temperature restrictions on the validity of the theory.

The work reported here builds on the previous work of Pesch and Kramer who computed the order parameter $\Delta(\vec{R})$ and the vector potential $\vec{A}(\vec{R})$ around a vortex in a superconductor.[11] All our numerical results are for a pure superconductor with the Ginzburg-Landau parameter $\kappa=0.9$ chosen by the above authors. The theory discussed here can be applied to the calculation of the free-energy change brought about by a defect in any surrounding self-consistent configuration of $\Delta(\vec{R})$ and $\vec{A}(\vec{R})$ to leading order in d^2/ξ_0^2. We can thus compute exactly, for small impurities, the free energy of an entire dilute distribution of impurities in a given $\Delta(\vec{R})$ and $\vec{A}(\vec{R})$. One could then try and solve the full summation problem in the presence of a random distribution of defects and a current by making an ansatz for the distortion of the vortex lattice, calculating the order parameter and vector potential field belonging to it without the impurities, then evaluating the change in free energy brought about by the presence of the impurities, and finally looking for the best ansatz. It seems too tedious, however, to have to do the full self-consistent $\Delta(\vec{R})$ and $\vec{A}(\vec{R})$ calculation from scratch for every tested bending and twisting of the vortex lattice. We therefore formulate an approximate but adequate set of simple rules for estimating the pinning potential of a defect at a given distance from a vortex line as a function of the temperature, temperature-independent coherence length, and the scattering properties of the defect. If the vortex lattice is not too dense and not too violently bent, this potential energy between a single vortex line and a single scattering center is not a bad starting point for calculating the optimum distortion of a vortex lattice torn between the pinning potential and the elastic deformation energy.

This paper is organized as follows. Section II introduces the quasiclassical theory as needed in the present context. The properties of the solutions of the transport-like equation are the subject of Sec. III in view of computing the Green's function numerically in an efficient fashion. Two simple examples are given of the quasiclassical method at work. Section IV is an account of our numerical procedures. Our results are given in Sec. V, and we compare them with experiment and discuss some generalization thereof in Sec. VI. Preliminary reports of parts of the present results have been published previously.[4,12]

II. QUASICLASSICAL FORMALISM

In the quasiclassical formalism, Green's functions appear in what is called the ξ-integrated form,

$$\hat{g}(\hat{k},\vec{R};\epsilon_n)=\int_{-E_c}^{+E_c} d\xi_k \hat{\tau}_3 \hat{G}(k\hat{k},\vec{R};\epsilon_n)\ , \tag{1}$$

where $\xi_k=\hbar v_F(k-k_F)$ is the normal-state quasiparticle energy near the Fermi surface, and the caret denotes a 2×2 Nambu matrix. $\hat{g}$ may be considered as the density matrix of quasiparticle excitations. The 2×2 matrix structure comes from the particle-hole degrees of freedom which form a two-dimensional Hilbert space. The symbols $\hat{\tau}_1$, $\hat{\tau}_2$, and $\hat{\tau}_3$ refer to the three Pauli matrices in the particle-hole space, and $\epsilon_n=(2n+1)\pi k_B T$ are the Matsubara frequencies. The integral in (1) is cut off at an energy E_c which is much larger than energies associated with the superfluid state $k_B T_c$, but much smaller than the Fermi energy E_F. The cutoff obviously shall appear in no physical quantities. It is in fact essential to the quasiclassical theory that there be the large gray area between the superfluid energies and the Fermi energy where the cutoff can be placed. The remaining variables in the quasiclassical Green's function, in addition to the Matsubara frequencies (energy variable), are the average position $\vec{R}$ of an excitation and the direction $\hat{k}$ of its wave vector (momentum).

In order for the quasiclassical Green's function to be useful at all, the equation of motion satisfied by the conventional Green's functions (Dyson's equation) has to be converted into an equation for the quasiclassical quantities. This has been achieved by Eilenberger,[9] and Larkin and Ovchinnikov.[10] We will first outline their scheme, which aims at the averaged properties of a superconductor with a random distribution of impurities, and then generalize it to describe local properties of a superconductor near a selected impurity (the pinning center).

The starting point is a Dyson equation together with a prescription for calculating the self energy $\hat{\Sigma}$ as a function of the Green's function.

$$(\hat{G}_0^{-1}-\hat{V}_{\rm imp}-\hat{\Sigma})\hat{G}=\hat{1}\ , \tag{2a}$$

$$\hat{\Sigma}=\hat{\Sigma}(\hat{G})\ . \tag{2b}$$

Here $\hat{G}_0$ is the free-electron Green's function in the presence of the magnetic field, and $\hat{V}_{\rm imp}$ is the impurity potential. $\hat{G}_0$ and $\hat{V}_{\rm imp}$ are to be understood as renormalized quantities which contain all high-energy and short-distance correlations that remain unchanged in the superconducting transition. Impurity averaging of Eq. (2a) leads to the replacement $\hat{V}_{\rm imp}\rightarrow\hat{\Sigma}_{\rm imp}$.

The self-energy can be expressed in terms of quasiclassical Green's functions by standard arguments based on the slow momentum variation of interaction and impurity vertices. The elimination of $\hat{G}$ from Dyson's equation (2a) in favor of the quasiclassical $\hat{g}$ can be carried out with the

aid of the so-called "left-right trick." The trick consists of subtracting, from Eq. (2a), the equivalent equation

$$\hat{G}(\hat{G}_0^{-1}-\hat{V}_{\rm imp}-\hat{\Sigma})=\hat{1}\ . \tag{2c}$$

After impurity averaging, one can neglect the weak k dependence of the factors $\hat{G}_0^{-1}-\hat{\Sigma}_{\rm imp}-\hat{\Sigma}$. Hence ξ_k integration of the difference only affects the factors $\hat{G}$ and turns them into quasiclassical $\hat{g}$. These steps lead to

$$\left[\left[i\epsilon_n+v_F\frac{e}{c}\hat{k}\cdot\vec{A}(\vec{R})\right]\hat{\tau}_3-\hat{\Delta}(\vec{R})-\hat{\sigma}_{\rm imp}(\hat{k},\vec{R};\epsilon_n),\hat{g}_{\rm imt}(\hat{k},\vec{R};\epsilon_n)\right]+i\hbar v_F\hat{k}\cdot\vec{\nabla}_{\vec{R}}\hat{g}_{\rm imt}(\hat{k},\vec{R};\epsilon_n)=0\ . \tag{3a}$$

We have called the Green's function $\hat{g}_{\rm imt}$ for intermediate, anticipating the effect of the separate pinning defect. All self-energies can be taken at the Fermi surface; we denote the Fermi-surface limit of $\hat{\Sigma}$ by $\hat{\sigma}$. Information has clearly been lost with the subtraction, and Eilenberger showed with his elegant operator trick that the essential part of it can be recovered through the normalization condition

$$\hat{g}_{\rm imt}^2(\hat{k},\vec{R};\epsilon_n)=-(\pi\hbar)^2\ . \tag{3b}$$

The square of the Green's function indicates matrix multiplication, and it is easy to see that the square is indeed conserved in Eq. (3a), the transportlike equation for the quasiclassical Green's function. The impurity self-energy which appears in Eq. (3a) is given as

$$\hat{\sigma}_{\rm imp}(\hat{k},\vec{R};\epsilon_n)=n\hat{t}_{\rm imp}(\hat{k},\hat{k},\vec{R};\epsilon_n)\ , \tag{4a}$$

where n is the density of impurities and $\hat{t}_{\rm imp}(\hat{k},\hat{k},\vec{R};\epsilon_n)$ is the forward-scattering limit of the single-impurity t matrix. The equation for $\hat{t}_{\rm imp}$ is

$$\hat{t}_{\rm imp}(\hat{k},\hat{k}',\vec{R};\epsilon_n)=v(\hat{k},\hat{k}')+\frac{N(0)}{\hbar}\int\frac{d^2k''}{4\pi}v(\hat{k},\hat{k}'')\hat{g}_{\rm imt}(\hat{k}'',\vec{R};\epsilon_n)\hat{t}_{\rm imp}(\hat{k}'',\hat{k}',\vec{R};\epsilon_n)\ . \tag{4b}$$

A very popular approximation in the theory of superconductivity is to truncate (4b) to second order in v (Born approximation). This yields

$$\hat{\sigma}_{\rm imp}(\hat{k},\vec{R};\epsilon_n)=n\frac{v_F}{2\pi}\int d^2q\frac{d\sigma}{d\Omega}(\hat{k},\hat{q})\hat{g}_{\rm imt}(\hat{q},\vec{R};\epsilon_n)\ . \tag{4c}$$

$d\sigma/d\Omega$ is the differential scattering cross section. We have dropped the irrevelant first-order term in v.

The order parameter or the off-diagonal self-energy $\hat{\Delta}(\vec{R})=i[\hat{\tau}_2{\rm Re}\Delta(\vec{R})+\hat{\tau}_1{\rm Im}\Delta(\vec{R})]$, and the vector potential in Eq. (3a) must obey the self-consistency conditions

$$\Delta(\vec{R})=N(0)V_{\rm BCS}\frac{k_BT}{\hbar}\sum_{n=-\infty}^{+\infty}\int\frac{d^2k}{4\pi}\tfrac{1}{2}{\rm tr}_2[\hat{g}(\hat{k},\vec{R};\epsilon_n)(\hat{\tau}_1-i\hat{\tau}_2)]\ , \tag{5a}$$

$$\frac{c\vec{\nabla}\times\vec{B}}{4\pi}=eN(0)\frac{k_BT}{\hbar}\sum_{n=-\infty}^{+\infty}\int\frac{d^2k}{4\pi}(v_F\hat{k}){\rm tr}_2[\hat{t}_3\hat{g}(\hat{k},\vec{R};\epsilon_n)]\ , \tag{5b}$$

where $\vec{B}=\vec{\nabla}\times\vec{A}$.

Equations (3)—(5) are a closed set, and they are also the ones that Pesch and Kramer[11] used in calculating the order parameter and the vector potential around a single vortex. The important fact to notice about Eq. (3a) is that it is a first-order ordinary differential equation, and hence it is quite easy to solve numerically.

The pinning impurity will now be introduced as a kind of additional boundary condition, or source term, in the transportlike equation. We will treat the pinning impurity separately from the rest, and average over the positions of all impurities except the priviledged one. This procedure is correct in the limit of long mean free path ($k_Fl\gg1$) as long as the pinning impurity is uncorrelated with the rest of the impurities. A set of mutually correlated impurities, such as a cluster of impurities or vacancies, have to be treated as a single defect in our scheme. There appears then a potential term $\hat{V}$ in the Hamiltonian describing the pinning center at $\vec{R}=\vec{r}$. $\hat{V}_{\rm imp}$ comprises the potentials of all other impurities. It is easy to see, in terms of the graphs in Fig. 1, that the full Green's function now obeys the equation

$$\hat{G}=\hat{G}_{\rm imt}+\hat{G}_{\rm imt}\hat{V}\hat{G}\ , \tag{6}$$

where $\hat{G}_{\rm imt}$ is the Green's function discussed above (except for the fact, of course, that the exact full Green's function appears in the self-energy equation). We want to express the scattering by our special pinning center via a t-matrix equation. This leads to the following set of equations:

$$(\hat{G}_0^{-1}-\hat{V}_{\rm imp}-\hat{\Sigma})\hat{G}_{\rm imt}=\hat{1}\ , \tag{7a}$$

$$\hat{\Sigma}=\hat{\Sigma}(\hat{G})\ , \tag{7b}$$

$$\hat{T}=\hat{V}+\hat{V}\hat{G}_{\rm imt}\hat{T}\ , \tag{7c}$$

$$\hat{G}=\hat{G}_{\rm imt}+\hat{G}_{\rm imt}\hat{T}\hat{G}_{\rm imt}\ . \tag{7d}$$

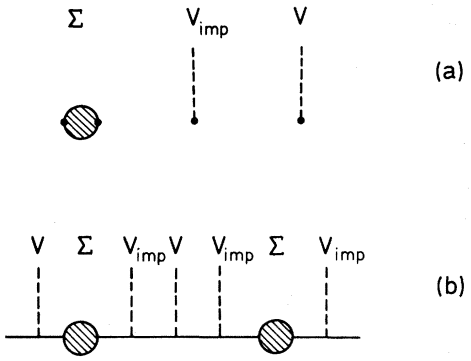

FIG. 1. Typical graph [labeled (b)] contributing to the Green's function $\hat{G}$ with self-energy insertions, impurity potentials, and localized potentials as shown in (a). $G_{\rm imt}$ is the Green's function with all orders and combinations of the self-energy insertion $\hat{\Sigma}$ and $\hat{V}_{\rm imp}$ included.

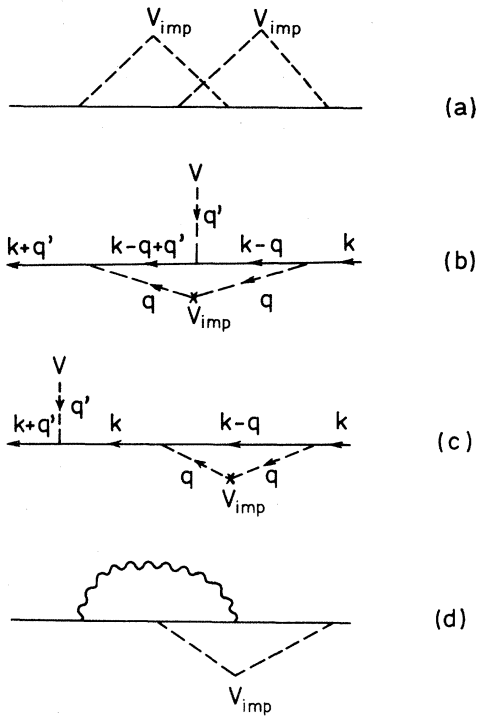

FIG. 2. Cross-linking diagrams between (a) two impurity potentials, (b) between an impurity potential and the special pinning potential, and (d) between an impurity potential and a self-energy insertion. Diagram (b) is to be compared with the non-cross-linking diagram (c). The momentum variables of each line are shown in (b) and (c). In (b) there is the additional requirement with respect to (c) that $\vec{k}-\vec{q}+\vec{q}\,'$ shall be in the thin shell around the Fermi surface.

Knowing $\hat{G}_{\rm imt}$, the t matrix can be calculated from Eq. (7c) and the exact Green's function from Eq. (7d).

Impurity averaging in the new set of equations proceeds as before with the additional observation that cross-linking diagrams between $V_{\rm imp}$ and V [Fig. 2(b)] can be neglected, with phase-space arguments similar to those leading to the discarding of the usual diagrams of the type of Fig. 2(a). Similar considerations apply to cross-linking impurity scattering and self-energy insertions.

The defect scattering potential V is to be understood again as being a phenomenological potential which, in principle, can be measured in the normal state of the metal and which varies slowly with the magnitude of the wave vector in the vicinity of the Fermi surface. The t-matrix equation, Eq. (7c), can therefore be simply ξ-integrated as it stands, the quasiclassical t matrix and the quasiclassical scattering potential being those of the normal state at the Fermi surface. Because of the pointlike nature ($d \ll \xi_0$) of the defect, the t matrix depends on $\hat{g}_{\rm imt}$ only at the site of the defect, $\vec{\mathbf{R}}=\vec{\mathbf{r}}$,

$$\hat{t}(\hat{k},\hat{k}';\epsilon_n)=v(\hat{k},\hat{k}')+\frac{N(0)}{\hbar}\int\frac{d^2\hat{k}}{4\pi}v(\hat{k},\hat{k}'')\hat{g}_{\rm imt}(\hat{k}'',\vec{\mathbf{R}}=\vec{\mathbf{r}};\epsilon_n)\hat{t}(\hat{k}'',\hat{k}';\epsilon_n)\ . \tag{8}$$

If one wishes to consider a larger defect, methods for solving for the t matrix for scattering off a surface are given by Buchholtz and Rainer.[13]

Equation (7d) can be ξ-integrated with the same left-right trick as above, and the result is identical with the exception of the source term on the right-hand side of the equation,

$$\left[\left[i\epsilon_n+v_F\frac{e}{c}\hat{k}\cdot\vec{\mathbf{A}}(\vec{\mathbf{R}})\right]\hat{\tau}_3-\hat{\Delta}(\vec{\mathbf{R}})-\hat{\sigma}_{\rm imp}(\hat{k},\vec{\mathbf{R}};\epsilon_n),\hat{g}(\hat{k},\vec{\mathbf{R}};\epsilon_n)\right]+i\hbar v_F\hat{k}\cdot\vec{\nabla}_{\vec{\mathbf{R}}}\hat{g}(\hat{k},\vec{\mathbf{R}};\epsilon_n)=[\hat{t}(\hat{k},\hat{k};\epsilon_n),\hat{g}_{\rm imt}(\hat{k},\vec{\mathbf{r}};\epsilon_n)]\delta(\vec{\mathbf{R}}-\vec{\mathbf{r}})\ . \tag{9}$$

The extra term causes a jump in the Green's function at the site of the defect.

Formally, one should require self-consistency according to Eqs. (5) in order for the theory to be complete. As we are interested in the free energy to lowest order in d^2/ξ_0^2 only, we do not have to require self-consistency of $\hat{g}$. The free energy due to the presence of the defect is then given as

$$\delta\Omega(\vec{\mathbf{r}})=N(0)\frac{k_BT}{\hbar}\int_0^1 d\lambda\sum_{n=-\infty}^{+\infty}\int\frac{d^2\hat{k}}{4\pi}\int d^3R\ {\rm tr}_2[\delta\hat{g}(\hat{k},\vec{\mathbf{R}};\epsilon_n;\lambda)\hat{\Delta}_b(\vec{\mathbf{R}})]\ , \tag{10}$$

as explained in Appendix A. Here $\delta\hat{g}=\hat{g}-\hat{g}_{\rm imt}$ must be evaluated at the order parameter $\hat{\Delta}(\vec{R})=\lambda\hat{\Delta}_b(\vec{R})$ and vector potential $\vec{A}_b(\vec{R})$, where the subscript b means order parameter and vector potential in the absence of the defect.

The procedure of calculating the free energy of a defect then consists of first computing $\hat{g}_{\rm imt}$ from Eq. (3) starting with some given self-consistent order parameter and vector potential field. The next step is solving the t-matrix equation, Eq. (8), and calculating the commutator to get the source term on the right-hand side of Eq. (9). Equation (9) then delivers $\hat{g}$, and therefore $\delta\hat{g}$, with which the free-energy change can be calculated according to Eq. (10).

The scattering properties of the defect enter via the potential $v(\hat{k},\hat{k}')$. It is natural to introduce a decomposition in spherical harmonics (for simplicity we consider isotropic systems with spherical defects) and scattering phase shifts δ_l (of the normal state at the Fermi surface),

$$v(\hat{k},\hat{k}')=\sum_{l,m} v_l Y_l^m(\hat{k}) Y_l^{m*}(\hat{k}') , \tag{11}$$

where $v_l=-[4/N(0)]\tan\delta_l$ and $Y_l^m(\hat{k})$ are the spherical harmonics. In the absence of information on the properties of a pinning defect, we use the hard-sphere phase shifts as a model,

$$\tan\delta_l=\frac{j_l(k_F d/2)}{n_l(k_F d/2)} , \tag{12}$$

where j_l and n_l are the Bessel and the Neumann functions of order l, and d is the diameter of the hard sphere. It turns out that at temperatures not too close to zero the phase shifts enter into the pinning potential through a particular combination, the transport (subscript tr) cross section, which is given by

$$\sigma_{\rm tr}=\frac{4\pi}{k_F^2}\sum_{l=0}^{\infty}(l+1)\sin^2(\delta_l-\delta_{l+1}) . \tag{13}$$

III. PROPERTIES OF THE SOLUTIONS

We note that the transportlike equation, comprised of Eqs. (3a) and (9), is a first-order ordinary differential equation along "trajectories" in the direction of the wave vector $\hat{k}$. The Matsubara frequencies and the four parameters necessary to specify a trajectory are parameters of the equation. In the case of an impure superconductor, the impurity self-energy couples the equations for the different trajectories. From now on we will only consider the pure superconductor, making the problem diagonal in all the parameters. The impure case needs somewhat more numerical effort and is so far unsolved.

It is shown in detail in Appendix B that the solution of the transportlike equation (3a) in a constant gap $\hat{\Delta}(\vec{R})=\hat{\Delta}$ and a vanishing vector potential is given as

$$\hat{g}=-\pi\hbar\frac{i\epsilon_n\hat{\tau}_3-\hat{\Delta}}{(\epsilon_n^2+|\Delta|^2)^{1/2}} \tag{14}$$

and it is also shown that the equation has two additional solutions, one exponentially growing and the other exponentially vanishing along the trajectory in the direction of the wave vector. The latter two solutions are given in Eq. (B4b).

Unbounded (exploding) solutions exist also when the gap varies in space. The physical solution is bounded, and special care is necessary in any numerical approach in order to avoid the admixture of unphysical exploding solutions. If one starts integrating the quasiclassical differential equations with some initial condition, the numerical solution is likely to blow up. Our numerical routine is tailored to take advantage of this. We construct the physical solution out of the numerically much easier accessible exploding solutions. The transportlike equation (3a) has the property that matrix multiplying any two of its solutions gives another solution. A simple example is the square of the physical solution which is proportional to the $\hat{1}$ matrix, and hence a trivial solution of (3a). One can show further that the physical solution is proportional to the commutator of two specially chosen exploding solutions. If we parametrize the position along the quasiclassical trajectory by x the special solutions are characterized by their limiting behaviors at $x\to\pm\infty$. One of them vanishes (exponentially) at $x\to+\infty$ and explodes (exponentially) at $x\to-\infty$, while the other does the converse. The commutator of these solutions is bounded at $x\to\pm\infty$ because the exponential decay and the exponential growth cancel. On the other hand, the only bounded solutions that exist are linear combinations of the physical solution and the unit matrix. Since the commutator has no unit component it must be proportional to the physical solution. In order to find the two exploding solutions numerically we integrate the transportlike equations along the trajectory towards the $\vec{R}$ point of interest, starting from each side of the point. If the starting points lie in an asymptotic region of constant order parameter, one can begin with the (analytically known) solution which vanishes in the appropriate direction, generating the exact exploding solutions. In practice one does not have to make sure that the exploding solutions are strictly vanishing in the reverse directions. It is sufficient to set out with some $\hat{g}$ at a number of factors $\hbar v_F/(\epsilon_n^2+\lambda^2|\Delta|^2)^{1/2}$ away from $\vec{R}$. The numerical result at $\vec{R}$ will then be dominated by the wanted solution because of its exponential growth in the direction the integration proceeds. The success of this method reflects the fact that superconducting system "forgets" in space over distances much larger than the coherence length.

The method of solution for $\hat{g}_{\rm imt}$ outlined above has the additional nice feature of giving directly the quantity $\delta\hat{g}$. The source term on the right-hand side of Eq. (9) forces a jump in the Green's function at the location of the defect. The extra bits in the function $\hat{g}$ constituting the jump have to be the solutions decaying one toward the left and the other toward the right. These are precisely the ones calculated above. The matrix giving the jump at the locality of the defect fixes uniquely the two constant coefficients multiplying the decaying solutions to give the correct $\delta\hat{g}$ appearing in Eq. (10).

As an illustration we shall calculate the free energy due to a defect in two simple cases. The details are given in

Appendix B. The first is the constant order parameter. The function $\hat{g}_{\rm imt}$ is then given by Eq. (14). The t-matrix equation, Eq. (8), together with Eq. (3b), reveals immediately that the t matrix can only have components proportional to $\hat{g}_{\rm imt}$ and the unit matrix, and the commutator on the right-hand side of Eq. (9) vanishes. We obtain a vanishing $\delta\hat{g}$; the impurity causes no change in the free energy of the system in accordance with Anderson's theorem.[14]

The second simple case is a model vortex with a vanishing core radius. The order parameter is then given by

$$\Delta(\rho,\psi,z)=\Delta e^{i\psi}\,, \tag{15}$$

where ρ, ψ, and z are the cylindrical coordinates, i.e., the vortex is parallel to the z axis at $\rho=0$. We calculate the pinning energy for a defect sitting directly at the vortex core. Then $\hat{k}\cdot\vec{A}=0$, since the only trajectories needed are those passing through the core. The order parameter is constant on both sides of the defect and the diverging solutions are given by Eqs. (B5) and (B6). Considering only s-wave scattering, solving the t matrix is trivial, and a straightforward application of the procedure described above leads to

$$\delta\Omega(\vec{r}=\vec{0})=-2k_BT\ln\cosh\left[\frac{\Delta\sin\delta_0}{2k_BT}\right]. \tag{16}$$

This result actually gives correctly the order of magnitude of the full pinning potential at not too high temperatures. One should observe that the result is negative, i.e., quasiparticle scattering brings about pinning. One can try and give a physical interpretation of the effect by noticing that the jump in the Green's function relaxes the requirement that the order parameter vanish at the core of the vortex. Equations (3) and (9) can be thought of as describing the propagation of whatever entities are described by the (anomalous) Green's function through the vortex core. At the vortex core there is the impossible requirement of the entities having to change their phase abruptly by π. Thus the vortex core leads to locally varying phases by Green's functions, or those entities, over a distance on the order of ξ_0 around a vortex. According to the BCS gap equation, such a state of affairs reduces $\Delta(\vec{R})$ or costs the system condensation energy. When a defect is added at the vortex core the entities are scattered to new directions where the phase change is less and the phase mismatch smaller. This physical picture explains quite nicely the order of magnitude of the effect, coherence length times the area, rather than the volume. Basically we are talking about the well-known effect that makes the coherence length of a dirty superconductor short. Scattering helps a superconductor to sustain changes in its order parameter.

IV. NUMERICAL SOLUTION

In general, a numerical calculation is required for the elementary pinning potential. Acccording to what was said in Sec. III, we only have to calculate, on both sides, the solution diverging toward the defect along the trajectory. The simplest numerical integration methods, such as the Runge-Kutta method, are adequate. As mentioned in the preceding section, it suffices to start the integration a few factors $\hbar v_F/(\epsilon_n^2+\lambda^2|\Delta|^2)^{1/2}$ away with, say, the constant-Δ solution diverging in the relevant direction. This means a few ξ_0 at worst, for small λ and $n=0$. The exploding solutions are enough to give us $\hat{g}_{\rm imt}$ at the defect. The final Green's function will look like

$$\hat{g}_{\rm imt}+c_l\hat{g}_l \tag{17}$$

on the left-hand side of the impurity, and

$$\hat{g}_{\rm imt}+c_r\hat{g}_r \tag{18}$$

on the right-hand side, where $\hat{g}_l$ and $\hat{g}_r$ are the diverging functions coming from the left- and from the right-hand side with $\hat{g}_{\rm imt}$ given, apart from normalization, as the commutator of the two. For a pointlike impurity the integration over $\vec{R}$ in Eq. (10) just turns out to be another integration along the trajectory, and it can be carried out simultaneously with the integration of the differential equations for the diverging solutions. The constants c_l and c_r must be determined after solving the t-matrix equation since they are determined by the jump. At the end those coefficients will multiply the integrals already stored. For each n and λ, several trajectories were calculated to obtain the spherical harmonics decomposition of $\hat{g}_{\rm imt}(\hat{k},\vec{r};\epsilon_n,\lambda)$ and for the final integration over $\hat{k}$ in Eq. (10).

For the t matrix we write

$$\hat{t}(\hat{k},\hat{k}';\epsilon_n,\lambda)=\sum_{l,m}\sum_{l',m'}\hat{t}_{lml'm'}(\epsilon_n,\lambda)Y_l^m(\hat{k})Y_{l'}^{m'*}(\hat{k}')\,, \tag{19}$$

and the t-matix equation, Eq. (8), then reduces to the matrix equation

$$\sum_{l,m}\hat{A}_{l''m''lm}(\epsilon_n,\lambda)\hat{t}_{lml'm'}(\epsilon_n,\lambda)=\delta_{l''l'}\delta_{m'',m'}v_{l'}\hat{1}\,, \tag{20}$$

with the coefficient matrix given by

$$\hat{A}_{lml'm'}(\epsilon_n,\lambda)=\delta_{l,l'}\delta_{m,m'}\hat{1}\frac{N(0)}{\hbar}v_l \times\int\frac{d^2\hat{k}}{4\pi}Y_l^{m*}(\hat{k})\hat{g}_{\rm imt}(\hat{k},\vec{R}=\vec{r};\epsilon_n)Y_{l'}^{m'}(\hat{k})\,. \tag{21}$$

As a result of the reflection symmetry of $\hat{g}_{\rm imt}$ with respect to the plane through the defect and perpendicular to the vortex line, $\hat{A}_{lml'm'}$ and $\hat{t}_{lml'm'}$ vanish if $l+m+l'+m'$ is odd, and Eq. (20) splits into two equations, one for $l+m$ even, the other for $l+m$ odd. The t matrix can then be calculated by inverting the two matrices A. The larger complex square matrix to be inverted has the dimension $(l+1)(l+2)$, which leads to a 30×30 matrix for $l=4$. The t matrix and $\hat{g}_{\rm imt}$ then give the commutator which fixes the jump of $\hat{g}$ at the defect, and this again determines the coefficients c_l and c_r of the integrals of $\Delta\hat{g}_l$ and $\Delta\hat{g}_r$ calculated previously. Finally everything has to be repeated for a number of n and λ. The sum with respect to n converges as $1/n^4$, and usually clearly less than ten n's are needed for an accurate extrapolation. Both the n sum and the λ integration grow more difficult at low temperatures. The contribution to $\delta\Omega$ apparently has an infinite slope at

$\lambda=0$ at $T=0$. For temperatures larger than $0.1T_c$, five λ points were sufficient. Below that temperature our numerical computation is no longer trustworthy.

We took the self-consistent $\Delta(\vec{R})$ and $\vec{A}(\vec{R})$ from the published data by Pesch and Kramer,[11] extrapolating $\Delta(\vec{R})$ according to $\Delta_\infty - c_1\exp(c_2R)/\sqrt{R}$. For the impurity at a distance r from the vortex, we needed the vector potential as well, which we extrapolated according to $\hbar c/2eR + c_3\exp(c_4R)/\sqrt{R}$. The extrapolation affects the result at the 10% level.

V. RESULTS

We now turn to the results of the numerical calculation for a pure superconductor, Ginzburg-Landau parameter $\kappa=0.9$, with a single vortex and a single impurity. In Fig. 3 the pinning potential with the defect right at the vortex is depicted as a function of the temperature for four different descriptions of the defect in terms of phase shifts. The zero-core vortex model is also given with s-wave unitary scattering and in the Born approximation. The results are normalized with the quantity $\xi_0\sigma_{tr}N(0)\Delta_0^2/2$. One sees that the pinning potential is proportional to ξ_0 multiplied by the area of the defect, rather than the volume of the defect, as in the old excluded volume effect. The second noteworthy feature of Fig. 3 is that the result is not affected by how the impurity is described in detail, apart from the unphysical divergence at $T=0$ of the Born approximation (if the scale had been chosen proportional to $\sqrt{\sigma}$ rather than σ, there would be no divergence). The zero-core vortex model differs from the others but is nevertheless a guide to the order of magnitude of the potential. The almost coinciding curves have been calculated for a real vortex in the Born approximation (curve W), and for three different sets of hard-sphere shifts reflecting the different radii $k_Fd/2=1$ (curve 1), $k_Fd/2=4$ (curve 4), and for the s-wave unitary limit $\delta_0=\pi/2$ (curve U).

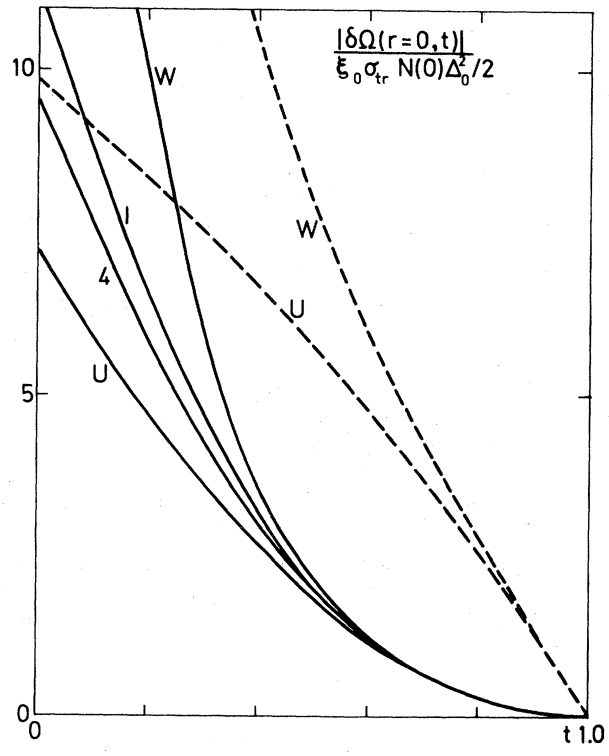

FIG. 3. Pinning energy as a function of the reduced temperature t (equal to T/T_c), the full curves for the s-wave unitary scattering (curve U), weak scattering ($k_Fd/2 \ll 1$) (curve W), and two different hard-sphere radii, $k_Fd/2=1.0$ (curve 1) and $k_Fd/2=4$ (curve 4). The dashed curves represent the zero-core-diameter model with the same symbols as defined above.

The region $T\sim T_c$, in particular, is determined by the transport cross section alone, and the individual phase shifts have some influence at low temperatures, just as in an analogous case in ^{3}He.[15,16] This is also evident in Fig. 4 where the pinning potential at $\vec{r}=0$ is displayed as a function of $k_Fd/2$, remembering that each d implies its own set of phase shifts. For $k_Fd/2>1$, the potential varies practically no more as a function $k_Fd/2$, and all the curves for different temperatures accumulate at $\delta\Omega$/normalization = 7.3 when $T\simeq T_c$. This practically agrees with the result (7.4) of the Ginzburg-Landau calculation (Figs. 5–7) based on the data of Pesch and Kramer[11] at $T=0.9T_c$. Thus the pinning potential scales, as a function of temperature, roughly as $(1-T/T_c)^2$.

Figures 5–7 display the pinning potential as a function of the distance of the defect from the vortex core at three different temperatures, $t=0.6$, 0.4, and 0.2 ($t=T/T_c$). Again, in each picture, the three different descriptions of the defect in terms of phase shifts mentioned above are displayed. In addition, there is a dashed line in each figure, identical in every one in terms of the scaling chosen in the picture. The dashed line is the prediction of the theory near the transition temperature. It can be calculated analytically.[17] For temperatures that are not too low the high-temperature theory agrees amazingly well with

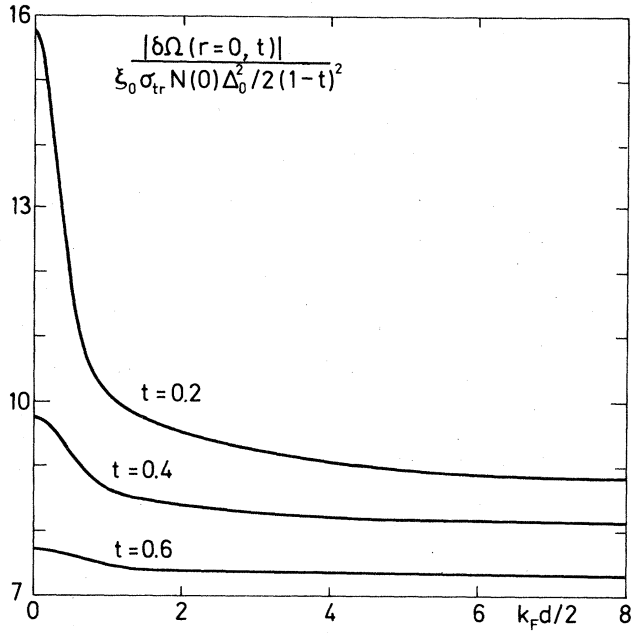

FIG. 4. Pinning energy normalized with $\xi_0\sigma_{tr}N(0)\Delta_0^2(1-t)^2/2$ as a function of the hard-sphere diameter d at three different temperatures, $t=0.2$, 0.4, and 0.6. Curves near T accumulate at the constant 7.3.

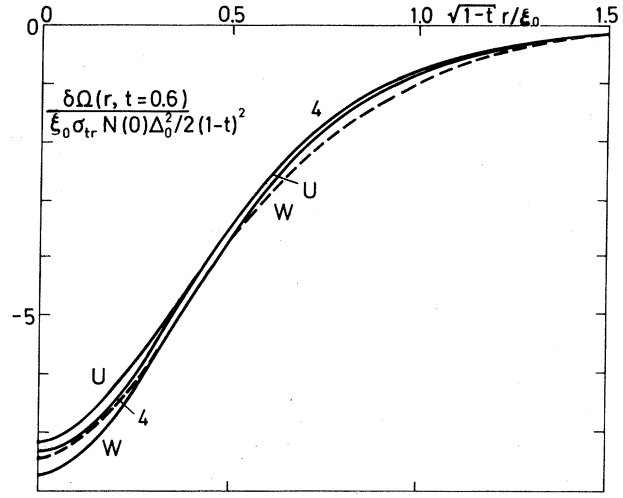

FIG. 5. Pinning potential as a function of the distance of the defect from the vortex core. The high-temperature approximation is drawn as a dashed line. The symbols labeling the curves are the same as in Fig. 3.

the full numerical results, implying that there is a nice "law of corresponding states" in terms of σ_{tr}, $(1-t)^2$, and $\xi_0/(1-t)^{1/2}$. Such a law is a handy tool comparing measurements with statistical summation theories. At the lowest temperatures the individual phase shifts play an increasingly important role. The hard-sphere phase shifts leads to a steeper potential at low temperatures than the high-temperature theory. The slope of the potential, giving the pinning force, reaches its maximum closer to the vortex and the maximum is higher by the factor 1.7 at our lowest temperature shown, $t=0.2$.

Returning to Fig. 3, one might make the observation that the pinning potential has a finite slope at $T=0$, i.e., the entropy is finite at $T=0$ which implies an unphysical

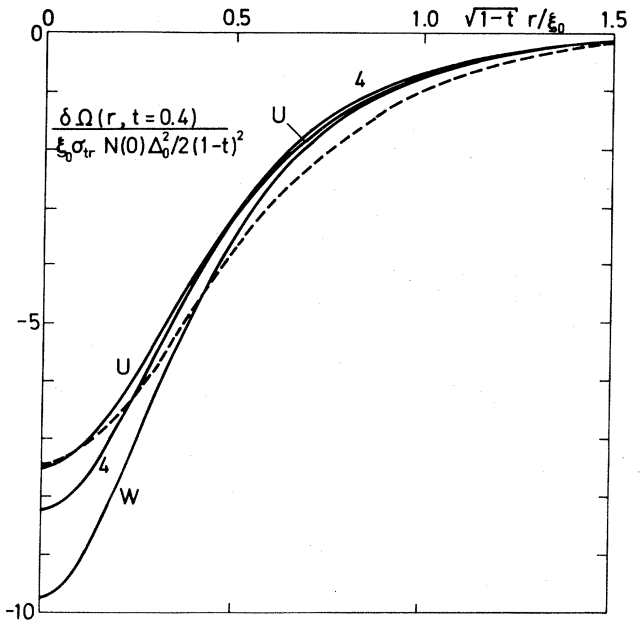

FIG. 6. Same as Fig. 5 at $t=0.4$.

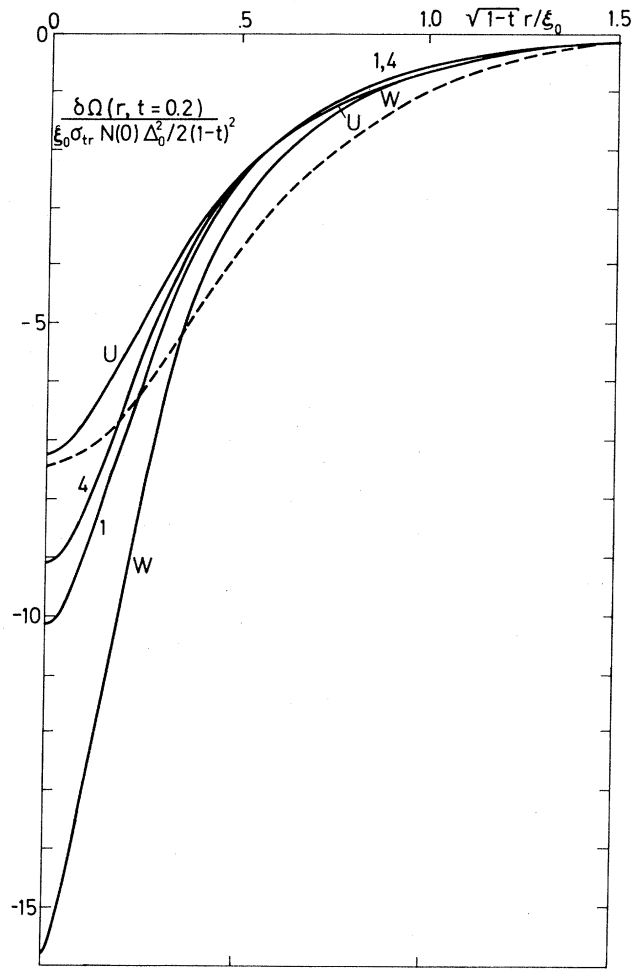

FIG. 7. Same as Fig. 5 at $t=0.2$.

degenerate ground state. In the zero-core-diameter model one can calculate the entropy at $T=0$ as $-d\delta\Omega/dT=-k_B\ln 4$. This result is an artifact of the quasiclassical theory: The quasiparticle bound states[18] around a vortex core at the tiny energy $\sim\Delta_0^2/E_F$ are put to exactly zero energy and counted as belonging to the ground state. The quasiclassical calculation is therefore only valid at temperatures larger than $T_c^2/T_F\simeq 10^{-4}T_c$. The pinning potential curves should flatten out below that temperature. This point is closely related to the fact that both the λ integral and the k integral become more critical at low temperatures. There is a divergency in $\hat{g}_{\text{imt}}$ at zero energy from the low-energy bound states. Computation is difficult already at $t=0.05$, and reliable results below that temperature would require a closer study of the problem. We in fact extrapolated the curves below $t=0.2$ in Fig. 3.

VI. DISCUSSION AND COMPARISON WITH EXPERIMENT

The results presented in the preceding section are, strictly speaking, for an isolated unbent vortex line. As already stressed in the Introduction, the present method of calculation is not restricted to this special case. The pinning energy can be calculated for an arbitrary field of $\Delta(\vec{R})$ and $\vec{A}(\vec{R})$.

In the presence of several defects with large separations on the atomic scale k_F^{-1}, the pinning potentials can be simply summed. If the quasiparticle mean free path l due to scattering from these defects falls below $\simeq\xi_0$, however, the averaged effect of the defects has to be taken into account in the impurity self-energy (4a). The difficult part of the multiple-defect problem is in the distortion of the vortex lattice, i.e., what shape the order parameter and vector potential fields take in the presence of the defects.

When the density of identical defects or impurities grows, the pinning potential of a single impurity is expected to grow smaller,[17] overwhelmed by the large amount of background scattering. The additional scattering renders the benefit of sticking to a given impurity smaller. Therefore the pinning potential decays as a function of the impurity parameter $\alpha=0.882\xi_0/l$ according to some power of $1/\alpha$. The numerical calculation is difficult, as explained in Sec. III. The maximum dissipationless current of the superconductor depends critically on the distribution of the scattering centers, clustering being the decisive factor.[6]

As to comparing our results with experiments, there seems to have been a problem about the pinning strength of small defects being too small,[1] as was already pointed out in the Introduction. More specifically, there are at least two experiments with small defects[19,20] to which the present theory should apply. Both suggest elementary pinning energies on the order we predict. Furthermore, Kerchner *et al.*[19] also find decreasing pinning with decreasing purity of the sample, in accordance with our expectation. There are experiments which suggest the opposite trend, however; see Ref. 19.

Only pointlike defects have been considered in detail in this paper. It is certainly legitimate, however, to somewhat generalize the physical picture according to which condensation energy lost in a vortex is partly recovered in a volume $\xi_0 d^2$ around a scattering center. If the defect is an entire line of scattering centers such as that represented by a dislocation, the vortex line tends to stick to such a line with an energy per unit of length proportional to the coherence length ξ_0 times the scattering strength of the line (strength per unit length). For a plane of scattering centers, such as a grain boundary, the energy per unit length of a sticking vortex line would go as ξ_0^2. This last prediction is in conflict with the result reported by Zerweck[21] and Yetter *et al.*[22] that pinning should vanish at the clean limit.

APPENDIX A

The starting point of the derivation of the free-energy expression, Eq. (10), is the general free-energy functional of Luttinger and Ward[23] supplemented by the magnetic field energy,[24]

$$\Omega(\hat{G},\hat{\Sigma},\hat{V},\lambda)=-\mathrm{Tr}[\lambda\hat{\Sigma}\hat{G}+\ln(-\hat{G}_0^{-1}+\hat{V}+\lambda\hat{\Sigma})]+\lambda\phi(\hat{G})+\int d^3R\frac{(\vec{\mathbf{B}}-\vec{\mathbf{B}}_a)^2}{8\pi}, \quad \text{(A1)}$$

where Tr stands for

$$\mathrm{Tr}[\cdots]=\frac{k_BT}{\hbar}\sum_{n=-\infty}^{+\infty}\int\frac{d^3k}{(2\pi)^3}\int d^3R\,\mathrm{tr}_2[\cdots], \quad \text{(A2)}$$

and the Green's function $\hat{G}$, the self-energy $\hat{\Sigma}$, and the external potential $\hat{V}$ may depend on the wave vector $\vec{\mathbf{k}}$, position $\vec{\mathbf{R}}$, and the Matsubara frequency ϵ_n. $\vec{\mathbf{B}}_a$ is the external magnetic field. An additional parameter λ has been introduced in Eq. (A1). The true energy corresponds to $\lambda=1$. $\phi(\hat{G})$ is defined diagrammatically so that $\delta\phi/\delta\hat{G}$ shall give the skeleton-diagram expansion of $\hat{\Sigma}$,

$$\delta\phi(\hat{G})=\mathrm{Tr}[\hat{\Sigma}\delta\hat{G}]. \quad \text{(A3)}$$

This property makes the free-energy functional stationary in $\hat{G}$. On the other hand, Ω is stationary in $\hat{\Sigma}$ as well because of Dyson's equation,

$$\hat{G}=(\hat{G}_0^{-1}-\hat{V}-\lambda\hat{\Sigma})^{-1}. \quad \text{(A4)}$$

The goal of the present exercise is a free-energy functional which depends only on quasiclassical quantities such as $\hat{g}$ and $\hat{\Delta}$. This can be achieved straightforwardly for the first term and the third term on the right-hand side of Eq. (A1). The logarithmic term can be handled by differentiating with respect to λ, after which the whole expression is directly ξ integrable, and then reintegrating over λ. The result is the quasiclassical free-energy functional,

$$\Omega-\Omega_{\mathrm{norm}}=\frac{k_BTN(0)}{\hbar}\int d^3R\sum_{n=-\infty}^{+\infty}\int\frac{d^2\hat{k}}{4\pi}\mathrm{tr}_2\left[-\hat{\sigma}(\hat{k},\vec{\mathbf{R}};\epsilon_n)\hat{g}(\hat{k},\vec{\mathbf{R}};\epsilon_n)+\int_0^1 d\lambda\,\hat{g}(\hat{k},\vec{\mathbf{R}};\epsilon_n,\lambda)\hat{\sigma}(\hat{k},\vec{\mathbf{R}};\epsilon_n)\right]+\phi(\hat{g}(\hat{k},\vec{\mathbf{R}};\epsilon_n))+\int d^3R\frac{(\vec{\mathbf{B}}-\vec{\mathbf{B}}_a)^2}{8\pi}. \quad \text{(A5)}$$

This functional is stationary at the physical solutions with respect to variations of the vector potential $\vec{\mathbf{A}}(\vec{\mathbf{R}})$, the self-energy $\hat{\sigma}(\hat{k},\vec{\mathbf{R}};\epsilon_n)$, and the Green's function $\hat{g}(\hat{k},\vec{\mathbf{R}};\epsilon_n)$. We emphasize that $\hat{g}(\hat{k},\vec{\mathbf{R}};\epsilon_n,\lambda)$ (Ref. 25) is a functional of $\hat{\sigma}$. The functional dependence is defined by the quasiclassical equations (9), (8), (3), and (4), with $\hat{\sigma}$ ($\hat{\sigma}\equiv\hat{\Delta}$ in our case) multiplied by λ. $\hat{g}(\hat{k},\vec{\mathbf{R}};\epsilon_n,\lambda)$ contains explicitly the effects of the privileged defect and the random impurities.

It is often convenient to eliminate the Green's function $\hat{g}(\hat{k},\vec{\mathbf{R}};\epsilon_n)$ by its stationarity condition, the BCS gap equation (5a). The free-energy functional then reduces to the functional used by Eilenberger:[24]

$$\Omega-\Omega_{\rm norm}=\frac{1}{V_{\rm BCS}}\int d^3R\,|\Delta(\vec{\mathbf{R}})|^2 + \frac{k_BTN(0)}{\hbar}\int d^3R\sum_{n=-\infty}^{+\infty}\int\frac{d^2k}{4\pi}\int_0^1 d\lambda\,\mathrm{tr}_2[\hat{g}(\hat{k},\vec{\mathbf{R}};\epsilon_n,\lambda)\hat{\Delta}(\vec{\mathbf{R}})]+\int d^3R\frac{(\vec{\mathbf{B}}-\vec{\mathbf{B}}_a)^2}{8\pi}\,. \tag{A6}$$

This result is very general and correct to all orders in d^2/ξ_0^2. In the present context we are only interested in the free energy to lowest order in d^2/ξ_0^2. The stationarity of Ω with respect to $\Delta(\vec{\mathbf{R}})$ and $\vec{\mathbf{A}}(\vec{\mathbf{R}})$ implies that any first-order changes in $\Delta(\vec{\mathbf{R}})$ and $\vec{\mathbf{A}}(\vec{\mathbf{R}})$ show up as second-order corrections in Ω. $\delta\Omega=\Omega(V)-\Omega(V=0)$ may be evaluated with the unperturbed $\Delta(\vec{\mathbf{R}})$ and $\vec{\mathbf{A}}(\vec{\mathbf{R}})$. In the subtraction only the second term in (A6) survives, and one obtains our formula (10) for the pinning energy.

APPENDIX B

In order to gain insight into the properties of the quasiclassical equations, here we shall explicitly write out, in matrix form, the coupled linear differential equations for the coefficients g_i in

$$\hat{g}=g_1\hat{\tau}_1+g_2\hat{\tau}_2+g_3\hat{\tau}_3\,, \tag{B1}$$

and study the properties of the solution in the two gap configurations mentioned in Sec. III, the constant gap and the zero-core model of a vortex. The gap matrix is written as

$$\hat{\Delta}=i(\Delta_1\hat{\tau}_1+\Delta_2\hat{\tau}_2)\,, \tag{B2}$$

where Δ_1 and Δ_2 are the imaginary and real parts of the complex gap. The function g_3 is the diagonal part of the Green's function in Nambu space; it is the only nonvanishing component of $\hat{g}$ in the normal state. The components g_1 and g_2 correspond to the anomalous part of the Green's function in the superfluid state.

Working out the commutators of the transportlike equation leads to the three coupled first-order differential equations ($x=\hat{k}\cdot\vec{\mathbf{R}}$)

$$\hbar v_F\frac{d}{dx}\begin{bmatrix}g_1\\g_2\\g_3\end{bmatrix}=2\times\begin{bmatrix}0 & i\epsilon_n+\frac{e}{c}v_F\hat{k}\cdot\vec{\mathbf{A}} & i\Delta_2\\ -i\epsilon_n-\frac{e}{c}v_F\hat{k}\cdot\vec{\mathbf{A}} & 0 & -i\Delta_1\\ -i\Delta_2 & i\Delta_1 & 0\end{bmatrix}\begin{bmatrix}g_1\\g_2\\g_3\end{bmatrix}. \tag{B3}$$

In order to understand some general properties of the solutions, we notice that there is a gauge for each trajectory which eliminates the vector potential from the coefficient matrix. Taking the order parameter to be constant in space, the eigenvalues of the Hermitian coefficient matrix are 0, 2α, and -2α with $\alpha=(\epsilon_n^2+\Delta_1^2+\Delta_2^2)^{1/2}$. The corresponding eigenvectors,

$$\hat{g}_0(x)=\pi\hbar\frac{i}{\alpha}\times\begin{bmatrix}\Delta_1\\\Delta_2\\-\epsilon_n\end{bmatrix}, \tag{B4a}$$

$$\hat{g}_\pm(x)=\begin{bmatrix}\mp\Delta_2\alpha+i\Delta_1\epsilon_n\\ \pm\Delta_1\alpha+i\Delta_2\epsilon_n\\ i(\Delta_1^2+\Delta_2^2)\end{bmatrix}e^{\pm 2\alpha x/\hbar v_F}\,, \tag{B4b}$$

are then a constant solution, an exponentially growing solution and an exponentially decaying solution. The constant solution has been normalized according to Eq. (3b), and it is clearly the physical solution. The normalization, according to Eq. (3b), of g_+ and g_- is equal to zero. In the general case the coefficient matrix varies with the coordinate along the trajectory.

It is easy to verify that the commutator of the matrix solutions $\hat{g}_+$ and $\hat{g}_-$ [Eq. (B4b)] gives the constant solution, Eq. (B4a). It is equally easy to understand that the t matrix arising from a constant and isotropic $\hat{g}_{\rm imt}$ commutes with $\hat{g}_{\rm imt}$, leading to no change in free energy from a defect in a constant-gap superconductor.

Another pinning problem which can be worked out in closed form is the zero-core vortex model with an s-wave scattering defect. We only need to consider trajectories in a single plane in which the vortex lies. The order parameter changes its phase abruptly by π at the vortex on all trajectories, but has its full amplitude everywhere. Let us call the part of the trajectory before hitting the vortex the left-hand side. Let the gap components on the left-hand side be $-\Delta_1$ and $-\Delta_2$. Then the purely diverging solution coming from the left-hand side is

$$\begin{bmatrix}+\Delta_2\alpha-i\Delta_1\epsilon_n\\ -\Delta_1\alpha-i\Delta_2\epsilon_n\\ \sim i(\Delta_1^2+\Delta_2^2)\end{bmatrix}e^{+2\alpha x/\hbar v_F}\quad\text{when } x\le 0\,. \tag{B5}$$

On the right-hand side the gap parameters have the opposite sign, and the diverging solution coming from the

right-hand side (or converging toward the right-hand side) is

$$\begin{bmatrix} +\Delta_2\alpha + i\Delta_1\epsilon_n \\ -\Delta_1\alpha + i\Delta_2\epsilon_n \\ i(\Delta_1^2+\Delta_2^2) \end{bmatrix} e^{-2\alpha x/\hbar v_F} \quad \text{when } x \geq 0 \, . \tag{B6}$$

The commutator of the two corresponding Nambu matrices gives the intermediate solution at the defect,

$$g_{\text{imt}}(x=0) = \frac{\pi\hbar}{\epsilon_n} \begin{bmatrix} -\Delta_2 \\ \Delta_1 \\ -i\alpha \end{bmatrix} . \tag{B7}$$

It may be an instructive exercise to verify Eq. (B7) by writing the Green's functions on the left- and right-hand sides as sums of the constant solution in each order parameter and solutions (B5) and (B6), respectively, multiplied with unknown coeffficients. Fitting the two at the vortex gives Eq. (B7).

It is now trivial to calculate the t-matrix for an s-wave scatterer $(v(\hat{k},\hat{k}') = v_0/4\pi = -[1/\pi N(0)]\tan\delta_0)$. We find, from, Eq. (8), that

$$\hat{t} = \frac{v_0}{4\pi} \frac{\hat{1} - i[N(0)/4]v_0(\epsilon_n^2+\Delta_1^2+\Delta_2^2)^{1/2}\hat{\tau}_3/\epsilon_n}{1+\{[N(0)/4]v_0(\epsilon_n^2+\Delta_1^2+\Delta_2^2)^{1/2}/\epsilon_n\}} , \tag{B8}$$

and the commutator $[\hat{t}, \hat{g}_{\text{imt}}]$ gives

$$[\hat{t}, \hat{g}_{\text{imt}}] = \frac{2i\hbar}{N(0)} \frac{\alpha \sin^2\delta_0}{\epsilon_n^2+(\Delta_1^2+\Delta_2^2)\sin^2\delta_0} \hat{\Delta} . \tag{B9}$$

As the jump will "heal" exponentially on both sides of the vortex (see Fig. 8 for a symbolic representation of what happens at the vortex), the integration of Eq. (10) over space results in

$$\int_{-\infty}^{+\infty} dx \, \text{tr}_2(\delta\hat{g}\hat{\Delta}) = -2\frac{\hbar}{N(0)} \frac{(\Delta_1^2+\Delta_2^2)\sin^2\delta_0}{\epsilon_n^2+(\Delta_1^2+\Delta_2^2)\sin^2\delta_0} , \tag{B10}$$

and

$$\delta\Omega = -2k_BT \int_0^1 d\lambda \sum_{n=-\infty}^{+\infty} \frac{\lambda(\Delta_1^2+\Delta_2^2)\sin^2\delta_0}{\epsilon_n^2+\lambda^2(\Delta_1^2+\Delta_2^2)\sin^2\delta_0} , \tag{B11}$$

which is easily integrated to give Eq. (16).

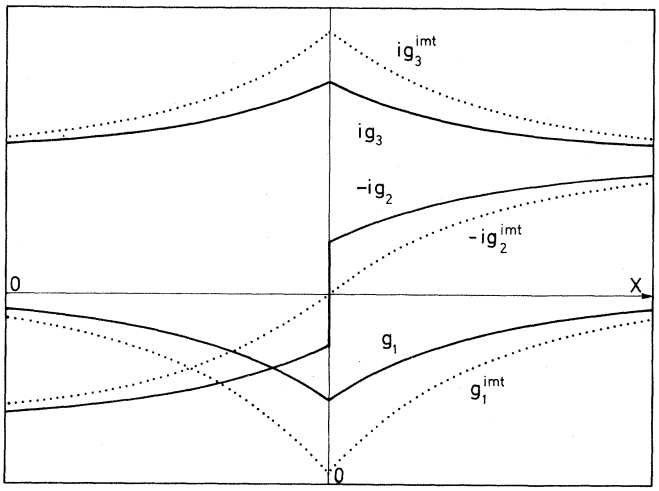

FIG. 8. Schematic plot of the intermediate Green's function (dotted line) and the Green's function in the presence of the defect at the vortex core (solid line) in the zero-core-diameter model. The gap has been chosen real, making g_1 real and g_2 and g_3 purely imaginary. Observe the jump of the anomalous Green's function g_2 at the defect.

*Present address.

[1]E. J. Kramer, J. Nucl. Mater. 72, 5 (1978).

[2]A. M. Campbell and J. E. Evetts, Adv. Phys. 21, 199 (1972).

[3]E. H. Brandt, J. Phys. (Paris) Colloq. 39, C6-1426 (1978).

[4]E. V. Thuneberg, J. Kurkijärvi, and D. Rainer, Phys. Rev. Lett. 48, 1853 (1982).

[5]H. Ullmaier, in *Irreversible Properties of Type II Superconductors,* Vol. 76 of *Springer Tracts in Modern Physics,* edited by G. Höhler (Springer, New York, 1975), p. 1.

[6]A. I. Larkin and Yu. N. Ovchinnikov, J. Low. Temp. Phys. 34, 409 (1979).

[7]H. R. Kerchner, J. Low Temp. Phys. 50, 337 (1983).

[8]E. H. Brandt, Phys. Rev. Lett. 50, 1599 (1983).

[9]G. Eilenberger, Z. Phys. 214, 195 (1968).

[10]A. I. Larkin and Yu. N. Ovchinnikov, Zh. Eksp. Teor. Fiz. 55, 2262 (1968) [Sov. Phys.—JETP 28, 1200 (1969)].

[11]W. Pesch and L. Kramer, J. Low Temp. Phys. 15, 367 (1974).

[12]J. Kurkijärvi, D. Rainer, and E. V. Thuneberg, in *Superconductivity in d- and f-Band Metals, 1982,* edited by W. Buckel and W. Weber (Kernforschungszentrum Karlsruhe, Karlsruhe, Federal Republic of Germany, 1982). In the figure of this reference the scale of distances is incorrent; the unit distance shown in terms of the chosen normalization should be 0.78.

[13]L. J. Bucholtz and D. Rainer, Z. Phys. B 35, 151 (1979).

[14]P. W. Anderson, J. Phys. Chem. Solids 11, 26 (1959).

[15]D. Rainer and M. Vuorio, J. Phys. C 10, 3093 (1977).

[16]E. V. Thuneberg, J. Kurkijärvi, and D. Rainer, J. Phys. C14, 5615 (1981).

[17]E. V. Thuneberg (unpublished).

[18]C. Caroli, P. G. de Gennes, and J. Martricon, Phys. Lett. 9, 307 (1964).

[19]H. R. Kerchner, D. K. Christen, C. E. Klabunde, S. T. Sekula, and R. R. Coltman, Jr., Phys. Rev. B 27, 5467 (1983).

[20]G. P. M. van der Mey and P. H. Kes (unpublished).

[21]G. Zerweck, J. Low Temp. Phys. 42, 1 (1981).

[22]W. E. Yetter, D. A. Thomas, and E. J. Kramer, Philos. Mag. B 46, 523 (1982).

[23]J. M. Luttinger and J. C. Ward, Phys. Rev. 118, 1417 (1960).

[24]G. Eilenberger, Phys. Rev. 153, 584 (1967).

[25]$\hat{g}(\hat{k},\vec{R};\epsilon_n,\lambda)$ should be carefully distinguished from $\hat{g}(\hat{k},\vec{R};\epsilon_n)$.